Dynamic and Steady State Behaviour of a Synchronous Reluctance Machine with leading Reactive Power through an Auxiliary winding

Ogunjuyigbe Ayodeji Samson Jimoh Adisa A Nicolae Dan Valentine
Department of Electrical and Electronic Engineering, Tshwane University of Technology
P.O.Box X680, Pretoria 0001. SOUTH AFRICA
aogunjuyigbe@yahoo.com, jimohaa@tut.ac.za , danaurel@yebo.co.za

***Abstract* – In attempt to improve the performance of synchronous reluctance machine the structure of the machine is modified to include an additional winding on the stator and injection of capacitance. This paper examines the dynamic and steady state behaviour of the modified machine based on its mathematical model and experiments performed on a practical prototype. The experimental results corroborate the solutions of the mathematical model as obtained through simulation. The modified machine shows significant improvement in performance over the conventional one.**

I. . INTRODUCTION

This paper is concerned about the dynamic and steady state behavior of a synchronous reluctance machine with a configuration that improves its performance. The synchronous reluctance machine is fitted with two three-phase stator windings- main and auxiliary windings, wound with the same pole numbers and a simple salient rotor structure. The machine has no rotor copper loss and consequently offers possibility of a good efficiency. The three phase main windings 'abc' carry the load current while the auxiliary windings 'xyz' are directly connected to a balanced capacitance for leading current injection. The conceptual diagram of the configuration is illustrated in Fig. 1. In a recent paper [1] the benefits of this configuration have been presented.

With the capacitance attached to the auxiliary winding, the machine operates at an improved power factor performance. Operation at good power factor that is uniquely achieved by the injection of leading current into the auxiliary winding, cumulated with the low manufacturing cost due to simple rotor construction will make such a machine structure attractive as a potential means of high speed , high power drive.

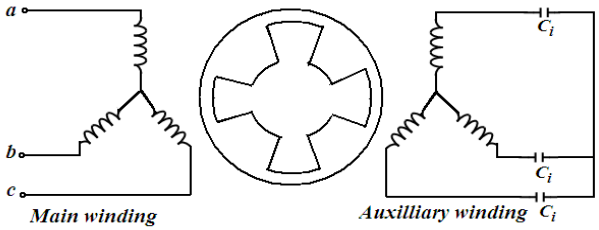

Fig. 1: Conceptual diagram for the stator windings and rotor structure of the machine.

This paper is organized as follows. Section II presents a detailed analysis of the development of the dq equations for this machine. An appropriate equivalent circuit based on these equations is developed. Simulation and experimental results describing the dynamic as well as the steady state performance of the machine are shown in section III and IV respectively. Further confirmatory steady state experimental results were presented in section V. The work is simply concluded in section VI. The simulation results were corroborated with the results obtained from an experimental machine.

II. . MACHINE MODEL

A. *Equivalent circuit*

In developing the model, classical assumptions were made so as to obtain closed form equations for machine inductances. A set of circuit differential equations describing the machine behaviour are written as:

$$[V_{abc}] = [R_{1s}][I_{abc}] + \tfrac{d}{dt}[\lambda_{abc}] \quad (1)$$

$$0 = [R_{2s}][I_{xyz}] + \tfrac{d}{dt}[\lambda_{xyz}] + [Vc_{xyz}] \quad (2)$$

where

$$[\lambda_{abc}] = [L_{abc}][I_{abc}] + [L_{abcxyz}][I_{xyz}] \quad (3)$$

$$[\lambda_{xyz}] = [L_{xyz}][I_{xyz}] + [L_{xyzabc}][I_{abc}] \quad (4)$$

The self and mutual inductances of equations (3) and (4) are evaluated using the method of winding functions [2, 3]. In this, if the inner radius of the stator is '*r*' , *l* is the effective magnetic length of the machine, and N_i, N_j are respectively the winding distribution function for winding 'abc' and 'xyz', then the inductance is given as :

$$L_{ij} = (\mu_o r l)\int g^{-1}(\phi,\theta_m) N_i(\phi,\theta_m) N_j(\phi,\theta_m) d\phi \quad (5)$$

where $g^{-1}(\phi,\theta_{rm})$ gives an approximation of the inverse air gap length.

Using equation (5), thirty-six machine inductances of equations (3) and (4) are obtained.

In order to predict the dynamic performance of the machine, equations (1) – (4) are solved simultaneously. However, they contain time varying parameters. Hence, in

order to reduce the complexity involved in resolving these equations, they are transformed to a dq rotating axis by multiplying them with an appropriate transformation matrix T(θ) to give:

$$[T(\theta)][V_{abc}] = [R_{1s}][T(\theta)][I_{abc}] + [T(\theta)]\tfrac{d}{dt}[\lambda_{abc}] \quad (6)$$

$$0 = [R_{2s}][T(\theta)][I_{xyz}] + [T(\theta)]\tfrac{d}{dt}[\lambda_{xyz}] + [T(\theta)][Vc_{xyz}] \quad (7)$$

Expanding these equations, and applying the chain rule technique, we obtain the qdo forms of the voltage and flux equations as written in equations (5)-(9):

$$[V_{qd01}] = [R_{1s}][I_{qdo1}] + \tfrac{d}{dt}[\lambda_{qd01}] - \omega[\lambda_{qd01}] \quad (5)$$

$$0 = [R_{2s}][I_{qdo2}] + \tfrac{d}{dt}[\lambda_{qd01}] - \omega[\lambda_{qd02}] + [V_{cqd0}] \quad (6)$$

$$[\lambda_{qd01}] = [L_{qd01}][I_{qd01}] + [L_{qd012}][I_{qd02}] \quad (7)$$

$$[\lambda_{qd02}] = [L_{qd021}][I_{qd01}] + [L_{qd02}][I_{qd02}] \quad (8)$$

where

$$\tfrac{d}{dt}[V_{cqdo}] = \tfrac{1}{C}[I_{Cqdo}] + \omega[V_{cqdo}] \quad (9)$$

Based on equations (5) - (8), the dq-equivalent circuit suitable for dynamic and steady state investigation is suggested as shown in Fig. 2.

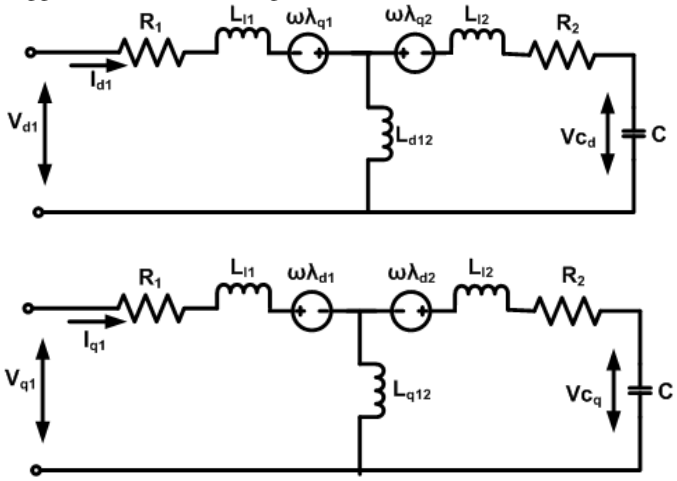

Fig. 2: The dq equivalent circuit of the synchronous machine with an auxiliary winding connected to a capacitor.

B. Electromagnetic Torque

Neglecting saturation, the electromagnetic torque can be expressed as the partial variation of the co-energy with respect to position as:

$$T_e = \mathrm{P_r} \times [i_{abcxyz}]^T \frac{\partial [L_{ss}]}{\partial \theta_r} [i_{abcxyz}] \quad (10)$$

Substituting the corresponding matrices and carrying out differentiation, equation (10) resolves to:

$$T_e = P_r L_{aa2}(I_{d1}I_{q1} + I_{d2}I_{q1} + I_{q2}I_{d1} + I_{q2}I_{d2}) \quad (11)$$

A key feature of equation (11) is that it contains additional components when compared to the torque equation of the conventional synchronous reluctance machine. This is indicative of the fact that the machine with the configuration described in this paper has a superior torque when compared to conventional synchronous reluctance machine. These additional torque terms of equation (11) represent the contribution as a result of the auxiliary winding that is connected to an external balanced capacitor. This is further confirmed with the measure results of section IV.

III. SIMULATION RESULTS

A computer model of the equivalent circuit of Fig. 2 built from equations (5) – (11) was developed in the Matlab/simulink environment. This was used to examine the dynamic behavior of this machine under different operating conditions. In the simulation, the main winding is connected to 50 Hz supply and the auxiliary winding is connected to a balanced capacitance to inject a leading current in the machine.

Also, in order to validate the computer model which has been developed, experimental tests were made on a prototype 2kW machine with parameters listed in table 1.

Free oscillation characteristics of the machine without and with 20μF compensation are respectively shown in Figs. 3 and 4. Fig. 3e and Fig.4e shows the measured phase current for the main winding without and with 20μF compensation. It is identical to the simulated results shown in Fig. 3b and 4b. This confirms the mathematical model and the correctness of the methodology developed.

A closer observation and comparison of Fig. 3 and 4 reveals the influence of the capacitor in the synchronization of the machine. Even though the magnitude of the starting current seems the same, it is obvious from the run up characteristics that the machine with compensation pull into synchronous operation faster at 0.5secs while the other only pull in at about 0.7secs. This only shows that the presence of capacitor also affect the starting, even though its presence may not be able to singly provide the induction torque required at starting to pull the machine into synchronism.

Ripples associated with synchronous reluctance machine are obvious in the torque waveforms of Fig.3c and 4c. However, the present configuration discussed here is found to greatly reduce the amplitude of the ripple torque.

Experimental as well as simulation results demonstrating the dynamic response of the modified machine to a step change in load from zero to 8.667Nm at 1.0 secs is illustrated in Fig.5. Similarly, with the loading of the machine in the laboratory environment, it was clearly observed that the rotor trembling as well as the noisy situation observed with the unmodified machine was rarely experienced with the configuration discussed here.

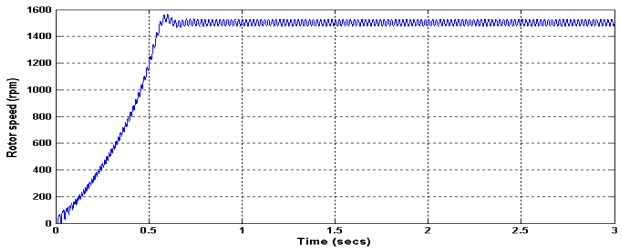

(a)

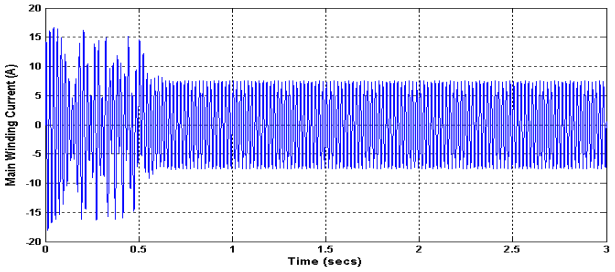

(b)

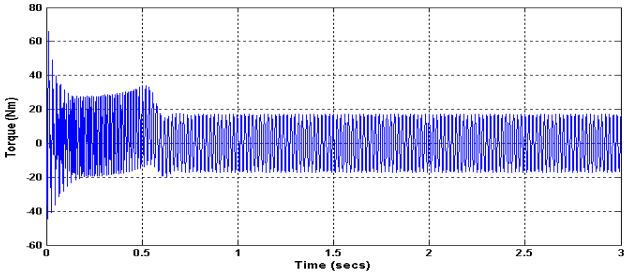

(c)

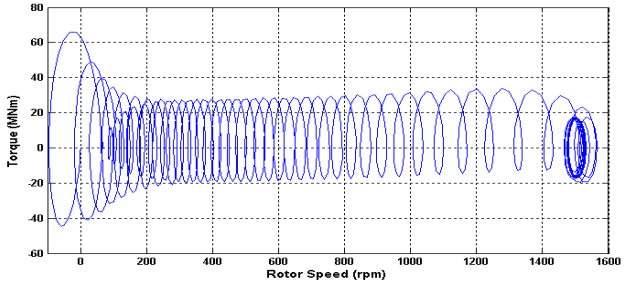

(d)

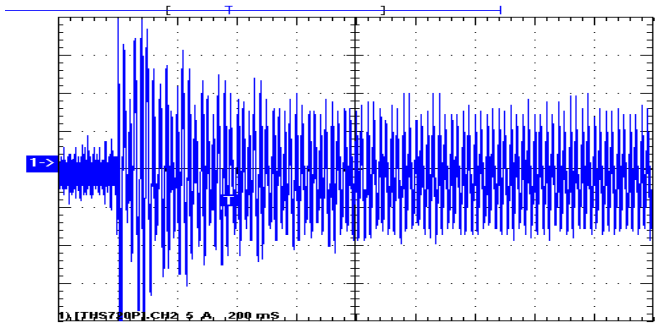

(e)

Fig. 3: Free oscillation characteristics of the machine without compensation. (a) Rotor speed, (b) Main winding current (c) Electromagnetic torque, (d) Torque vs speed (e) Experimental measurement of main winding current (vertical-5A/div, Hor. 200ms/div)..

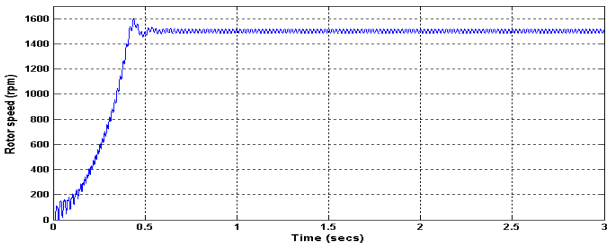

(a)

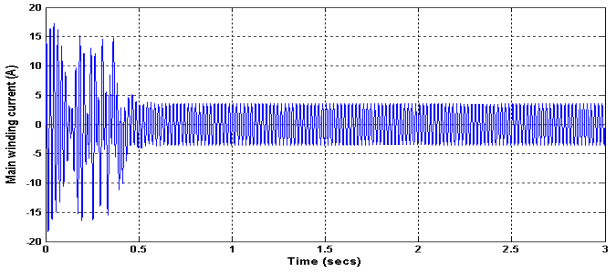

(b)

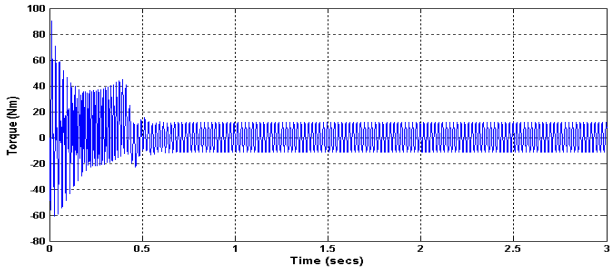

(c)

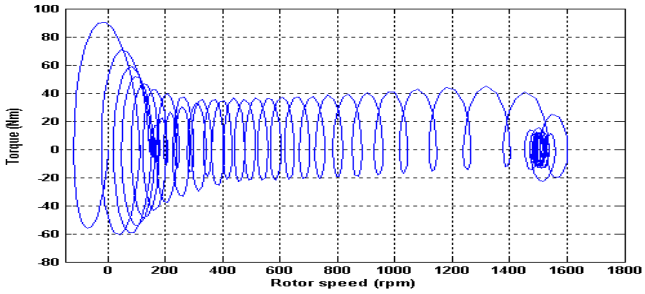

(d)

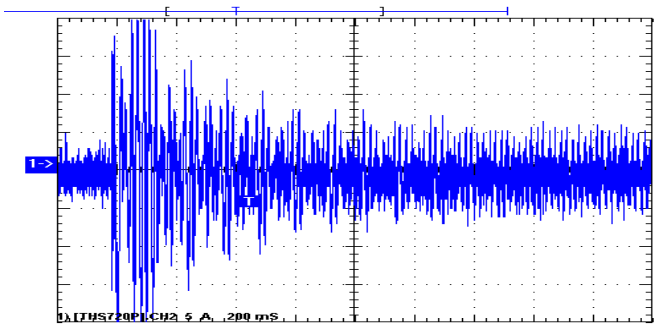

(e)

Fig. 4: Free oscillation characteristics of the machine with 20μF compensation. (a) Rotor speed, (b) Main winding current, (c) Electromagnetic torque, (d) Torque vs speed (e) Experimental measurement of main winding current (vertical-5A/div, Hor. 200ms/div).

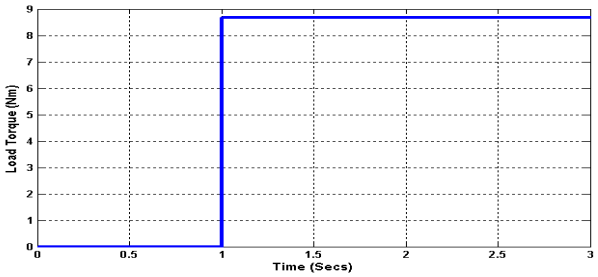

(a)

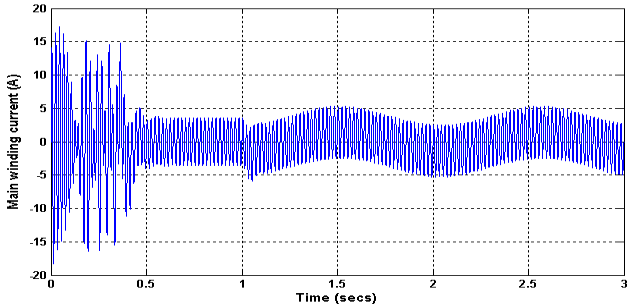

(b)

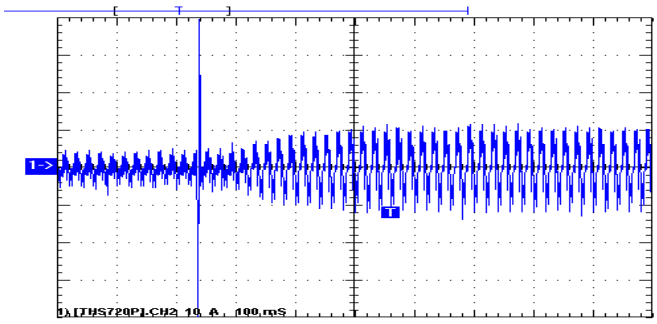

(c)

Fig. 5: Dynamic response of the modified machine to a step change in load from zero to 8.667Nm. (a) Load step, (b) Main winding current, (c) Experimental measurement of main winding current (vertical-10A/div, Hor. - 100ms/div).

IV. Steady State Analysis

Under steady state condition, the state derivatives in equations (5) – (9) are set zero [6]. The resulting steady state equations with little rearrangement will yield an equivalent circuit of the form shown in Fig. 5.

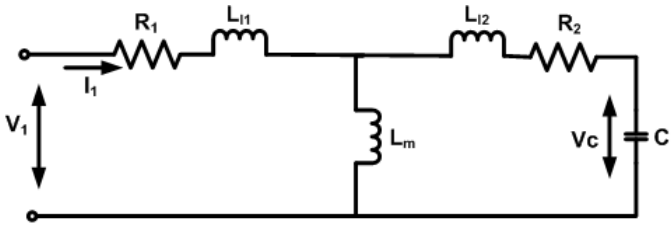

Fig. 5: Per phase steady state equivalent circuit of the synchronous machine with an auxiliary winding connected to a capacitor.

The per phase equivalent circuit is then used to examine the performance characteristics of the machine. The total per phase equivalent impedance (Z_{eq}) of the machine when viewed from the source can be expressed as:

$$Z_{eq} = \mathrm{R}_{eq} + jX_{eq} \tag{12}$$

where R_{eq} and X_{eq} are respectively the effective resistance and reactance of the circuit. The saliency presented by the rotor of the machine is well manifested in the expression for the inductances of the equivalent circuit [1, 4].

A. *Electromagnetic Torque*

Using the measured parameters of the experimental machine as shown in Table 1, the variation of the steady state torque as a function of the load angle is shown in Fig. 6 for different values of capacitor, while a contour plot of the measured torque as a function of capacitance and load angle is shown in Fig. 7. Also, the torque characteristic of the conventional machine without an auxiliary winding is shown in Fig. 6. It became essentially obvious from these figures that the relative torque improvement introduced by the configuration discussed in this work is only beyond a load angle of 15°. This is basically for the experimental machine with the parameters listed in Table 1. Illustrating with 25µF compensation, at a load angle of about 25°, the machine with the new configuration presents a torque improvement of about 16.16%.

TABLE I: SPECIFICATIONS OF THE MACHINE

Phase voltage	150V
Frequency	50 Hz
Poles	4
Direct axis reactance	43.41Ω
Quadracture axis reactance	12.60Ω
Main winding resistance	4.766Ω
Auxiliary winding resistance	18.76Ω
No of slots	36
Number of turns per coil	45

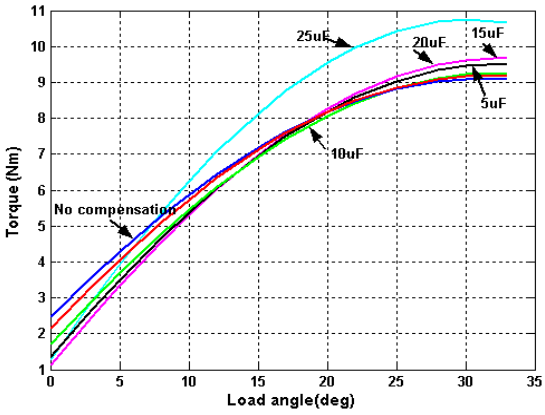

Fig. 6: Steady state torque (obtained from measured parameters) as a function of load angle for the synchronous reluctance machine with and without auxiliary winding connected to capacitor.

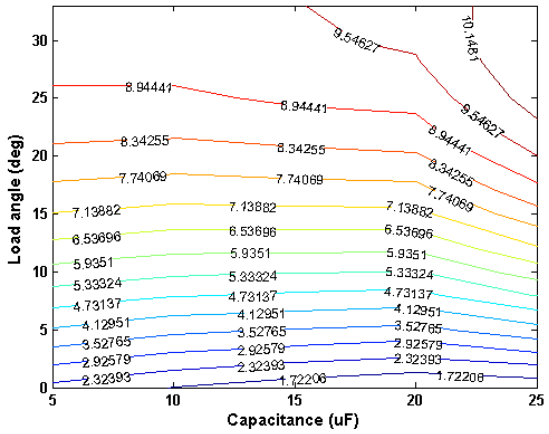

Fig. 7: Contour plot of torque (obtained from measured parameters) of the synchronous reluctance machine with an auxiliary winding connected to a capacitor as a function of load angle and capacitance.

B. Power Factor

The power factor performance of the machine as evaluated from the equivalent circuit of Fig. 5 can be expressed as:

$$\cos\phi = \frac{R_{eq}}{\sqrt{R_{eq}^2 + X_{eq}^2}} \tag{14}$$

The power factor for the experimental machine with a 20μF capacitor connected to the auxiliary winding were calculated for different load angles and compared with experimental results in Fig. 8. The figure also displays the calculated as well as measured power factors of the conventional machine. A good correlation between the calculated and experiments is achieved.

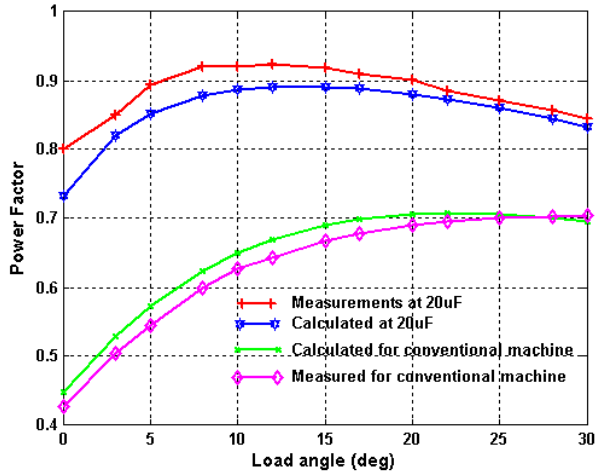

Fig. 8: Measured and calculated power factor of the machine (**with and without auxiliary winding connected to a capacitor**) as a function of the load angle.

It can be seen that unlike the conventional reluctance machine with a maximum power factor of 0.705, a power factor of 0.923 was achieved with the synchronous reluctance machine having the configuration discussed in this paper. Furthermore, the modified machine also provide relatively high power factor over the range of operational load angles. This is due to the presence of the auxiliary winding and the capacitance attached to it for the injection of leading current into the machine.

V. EXPERIMENTAL RESULTS

Two full pitch, single layer coils were wound in the stator frame DZ112M of a squirrel cage induction machine. The auxiliary winding was however wound using wires of thinner diameter so that the stator slot will be able to accommodate the two sets of winding. The rotor is of the simple salient type. The particular machine used for the experiment validation is a cage reluctance synchronous motor. The picture of the experimental set up is shown in Fig. 9.

Fig. 10 shows the waveform of the leading current injected into the machine as a result of the capacitance that is attached to the auxiliary winding, while Fig. 11 shows the test results of the main winding voltage and current at a load angle of 20° with 20μF compensation. This test result waveform is indicative of the good compensation obtained with the capacitance attached to the auxiliary winding. It also corroborates the curves earlier presented in Fig. 8. However, some level of harmonics was noticed in the current waveform, but the percentage of harmonics measured with the modified machine was found to be much lower when compared to that of the machine without compensation. The harmonics can be primarily adduced to the type of rotor used in this experiment.

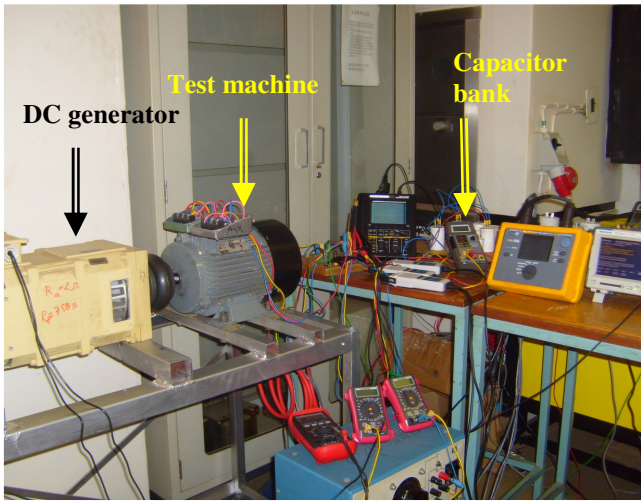

Fig. 9: Pictorial view of the experimental setup

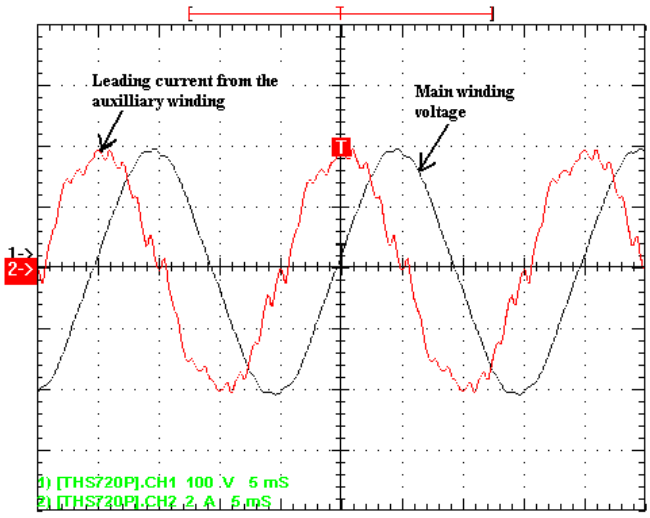

Fig. 10: Waveforms of the motor under load (δ=20°) with 20μF compensation. Red: Leading current of the auxiliary winding (2A/div); Black: Voltage in the main winding (100V/div).

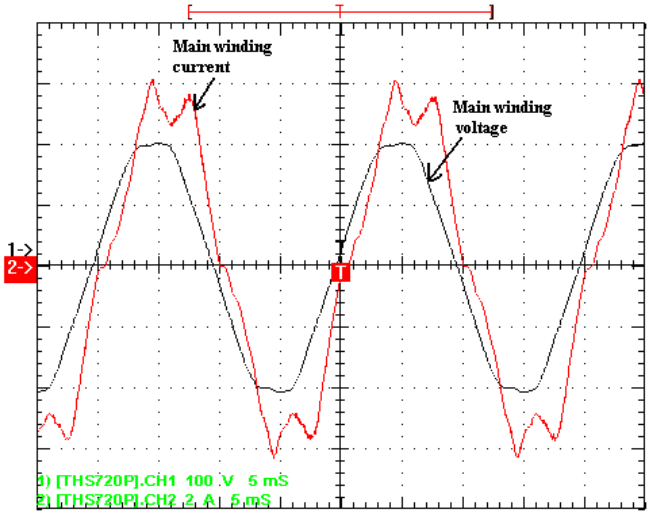

Fig. 11: Waveforms of the motor under load (δ=20°) with 20μF compensation. Red: Main winding current (2A/div); Black: Voltage in the main winding (100V/div).

VI. Conclusion

In this paper, a detailed analysis of the development of the dq model and equivalent circuit for an improved synchronous reluctance machine with capacitance injection through an auxiliary winding has been presented. The modelling equations (derived in the dq rotor reference frame) for this machine as well as the steady state analysis showed a superior torque and power factor performance by the synchronous reluctance machine with an auxiliary winding connected to balanced capacitance when compared to the conventional reluctance machine. Simulation results showing the dynamic as well as the steady state response of this machine were well corroborated with experimental measurements. This confirms the mathematical model and the correctness of the methodology developed. With the known advantages presented by synchronous reluctance machine, the configuration discussed in this paper is expected to widen the application area. This configuration will also find a general application in high power synchronous drives.

VII. References

[1] Ogunjuyigbe A.S.O, Jimoh, A.A, and Nicolae, D.V, "Improving Synchronous Reluctance machine performance by direct capacitance injection through an Auxiliary winding" *Proceedings of the International Conference on Electrical Machines and Systems ICEMS* 2007, paper IMP-05, pp.1055-1060.

[2] Novotny D.W and Lipo, T.A. *Vector Control and Dynamics of AC drives.* Claderon Press. 2000.

[3] Ojo. O, Gan Dong, and M.O. Omoigui, "Analysis of a Synchronous Reluctance Machine with an Auxiliary Single-Phase Winding" *IEEE Transactions on Industry Applications*, Vol. 39, No. 5 Sept/Oct. 2003. pp 1307-1313.

[4] Bertz, R.E. et al. "Control of Synchronous Reluctance Machines" *IEEE Transactions on Industry Applications*, Vol. 29, No. 6. 1993. pp. 1110-1122.

[5] Boldea I., Fu, X.Z., and Nasar, S.A. *.Performance Evaluation of Axially Laminated Anisotropic (ALA) Rotor Reluctance Synchronous Motors.* IEEE Transactions on Industrial applications, Vol. 30, No 4. pp. 977-985, 1994.

[6] P.C. Krause '*Analysis of Electric Machinery'* McGraw-Hill Book Company, 1986.

[7] E.S Obe, and T. Senjyu, "Analysis of a polyphase synchronous reluctance motor with two identical stator windings*" EPSR 76*. 2005, pp 515-524.

[8] Matsuo, T and Lipo, T.A, "Rotor Design Optimisation of Synchronous Reluctance Machine*". IEEE Transaction on Energy Conversion,* Vol. 9, No.2, pp 359-365.